Gill morphology and acute hypoxia: responses of mitochondria-rich, pavement, and mucous cells in the Amazonian oscar (*Astronotus ocellatus*) and the rainbow trout (*Oncorhynchus mykiss*), two species with very different approaches to the osmo-respiratory compromise

Victoria Matey, Fathima I. Iftikar, Gudrun De Boeck, Graham R. Scott, Katherine A. Sloman, Vera M.F. Almeida-Val, Adalberto L. Val, and Chris M. Wood

Abstract: The hypoxia-intolerant rainbow trout (*Oncorhynchus mykiss* (Walbaum, 1792)) exhibits increased branchial ion permeability and Na^+ influx during acute exposure to moderate hypoxia (P_{O_2} = 80 torr; 1 torr = 133.3224 Pa), manifesting the usual trade-off between gas exchange and electrolyte conservation. In contrast, the hypoxia-tolerant oscar (*Astronotus ocellatus* (Agassiz, 1831)) is unusual in exhibiting decreased branchial ion permeability to ions and Na^+ influx during acute exposure to severe hypoxia (P_{O_2} = 10–20 torr). These different physiological approaches to the osmo-respiratory compromise correlate with rapid, oppositely directed changes in gill morphology. In oscar, pavement cells (PVCs) expanded, partially covering neighboring mitochondria-rich cells (MRCs), which were recessed and reduced in size. Those remaining open were transformed from "shallow-basin" to "deep-hole" forms with smaller openings, deeper apical crypts, and smaller numbers of subapical microvesicles, changes that were largely reversed during normoxic recovery. In contrast, moderate hypoxia caused outward bulging of MRCs in rainbow trout with increases in size, surface exposure, and number of subapical microvesicles, accompanied by PVC retraction. These changes were partially reversed during normoxic recovery. In both rainbow trout and oscar, hypoxia caused discharge of mucus from enlarged mucous cells (MCs). Rapid, divergent morphological changes play an important role in explaining two very different physiological approaches to the osmo-respiratory compromise.

Résumé : La truite arc-en-ciel (*Oncorhynchus mykiss* (Walbaum, 1792)) qui est intolérante à l'hypoxie montre une perméabilité branchiale accrue aux ions et un influx de Na^+ durant une exposition aiguë à une hypoxie modérée (P_{O_2} = 80 torr; 1 torr = 133.3224 Pa), ce qui représente le compromis habituel entre les échanges gazeux et la conservation des électrolytes. À l'opposé, l'oscar (*Astronotus ocellatus* (Agassiz, 1831)), qui est tolérant à l'hypoxie, réagit de façon inhabituelle par une diminution de la perméabilité des branchies aux ions et de l'influx de Na^+ durant une exposition aiguë à une hypoxie sévère (P_{O_2} = 10–20 torr). Il y a une corrélation entre ces approches physiologiques différentes au compromis osmo-respiratoire et les changements rapides de la morphologie des branchies dans des directions opposées. Chez l'oscar, les cellules pavimenteuses (PVC) prennent de l'expansion et couvrent partiellement les cellules riches en mitochondries (MRC) voisines qui se rétractent et rapetissent. Celles qui restent ouvertes se transforment d'une forme de « bassin évasé » à une de « dépression profonde » avec des ouvertures réduites, de cryptes apicales plus accentuées et un nombre restreint de microvésicules subapicales, des modifications qui en grande partie régressent durant le rétablissement de la normoxie. Au contraire, l'hypoxie modérée chez la truite arc-en-ciel cause un ballonnement des MRC vers l'extérieur et une augmentation de taille, de la surface d'exposition et du nombre de vésicules subapicales, ainsi qu'un retrait des PVC. Ces changements régressent

Received 16 April 2010. Accepted 11 January 2011. Published at www.nrcresearchpress.com/cjz on 12 April 2011.

V. Matey. Department of Biology, Center for Inland Waters, San Diego State University, San Diego, CA 92182-4614, USA.
F.I. Iftikar. Department of Biology, McMaster University, Hamilton, ON L8S 4K1, Canada.
G. De Boeck. Department of Biology, University of Antwerp, Groenenborgerlaan 171, B-2020 Antwerp, Belgium.
G.R. Scott. Department of Zoology, University of British Columbia, Vancouver, BC V6T 1Z4, Canada.
K.A. Sloman. School of Sciences, University of West of Scotland, Paisley, Scotland, PA1 2BE, UK.
V.M.F. Almeida-Val and A.L. Val. Laboratory of Ecophysiology and Molecular Evolution, Instituto Nacional de Pesquisas da Amazônia (INPA), Manaus, Brazil.
C.M. Wood. Department of Biology, McMaster University, Hamilton, ON L8S 4K1, Canada; Division of Marine Biology and Fisheries, Rosenstiel School of Marine and Atmospheric Science, University of Miami, Miami, FL 33149, USA.

Corresponding author: V. Matey (e-mail: kuperman@sunstroke.sdsu.edu).

partiellement durant la récupération normoxique. Tant chez la truite arc-en-ciel que chez l'oscar, l'hypoxie provoque une sécrétion de mucus par les cellules à mucus (MC) élargies. Ces changements morphologiques rapides et divergents jouent un rôle important et expliquent les deux approches très différentes au compromis osmo-respiratoire.

[Traduit par la Rédaction]

Introduction

The fish gill is the basic site of respiration, ionic regulation, acid–base regulation, and excretion of nitrogenous wastes (Laurent 1984; Wilson and Laurent 2002; Evans et al. 2005). Three main cell types are present on the gill surface. Whereas mitochondria-rich cells (MRCs) have been generally well studied, much less is known about pavement cells (PVCs) and mucous cells (MCs). MRCs normally represent <15% of the cells in the branchial epithelium, but are generally agreed to play a central role in ion regulation (Perry 1997; Marshall 2002; Evans et al. 2005; Kaneko et al. 2008). Alterations in the number and distribution of MRCs within the gill epithelium of freshwater fish have been observed in response to a variety of environmental stressors (Laurent and Perry 1991; Goss et al. 1995). PVCs cover about 90% of the branchial epithelium and their major function is generally considered to be gas exchange. However, the presence of an apically located proton pump, V–H^+–ATPase, indicates they may also contribute to Na^+ uptake (Laurent et al. 1994; Perry 1997; Wilson et al. 2000; Marshall 2002). PVCs have large polygonal surfaces covered by microridges generated by folds of the apical membrane. These may serve to anchor mucus on the epithelial surface (Moron et al. 2009). They also increase gill surface area by more than twofold (Olson and Fromm 1973), providing a reserve of apical membrane (Avella et al. 2009) that allows them to expand or shrink, covering and uncovering adjacent MRCs and MCs in various circumstances (Goss et al. 1994; Daborn et al. 2001; Matey et al. 2008). MCs are low in numbers but are thought to play an important protective role (Shephard 1994). Environmental stressors cause the release of stored mucous granules by exocytosis, and gel-like mucus spreads along the gills (Verdugo 1991). This highly anionic, negatively charged medium may contribute indirectly to ion uptake by creating a microenvironment rich in cations, which is thought to facilitate active uptake and decrease passive ion loss (Handy 1989; Shephard 1994; Roberts and Powell 2003; Moron et al. 2009).

The functional trade-off between two of the key branchial functions, respiratory gas exchange and ionic regulation, has been termed the osmo-respiratory compromise (Nilsson 2007). This was originally studied in the context of exercise, where numerous investigations have demonstrated that when freshwater fish increase effective branchial permeability and surface area to exchange more O_2 and CO_2 during active swimming, they lose ions and gain water, and eventually implement compensatory measures (Randall et al. 1972; Wood and Randall 1973*a*, 1973*b*; Hofmann and Butler 1979; Gonzalez and McDonald 1992, 1994; Postlethwaite and McDonald 1995). More recently, this same trade-off has been studied in the context of the respiratory limitations caused by proliferation of MRCs in the branchial epithelium (Greco et al. 1995, 1996; Henriksson et al. 2008). Another aspect is the spectacular "remodeling" of the gill macrostructure that certain cyprinids such as the Crucian carp (*Carassius carassius* (L., 1758)) (Sollid et al. 2003, 2005; Sollid and Nilsson 2006; Nilsson 2007), goldfish (*Carassius auratus* (L., 1758)) (Sollid et al. 2005; Mitrovic and Perry 2009, Mitrovic et al. 2009), and scaleless carp (*Gymnocypris przewalskii* (Kessler, 1876)) (Matey et al. 2008) implement when exposed to chronic hypoxia or high temperatures. These fish appear to "grow lamellae" by losing interlamellar masses so as to gain surface area for gas exchange.

Recently, we have characterized the osmo-respiratory compromise in another context, during the responses to acute hypoxia of two noncyprinid teleosts that belong to quite distant phylogenetic groups. The Amazonian oscar (*Astronotus ocellatus* (Agassiz, 1831)) (local common name Acará-açu) is a cichlid that routinely encounters severe hypoxia in its natural habitat and is extremely tolerant, surviving P_{O_2} levels <30 torr (1 torr = 133.3224 Pa) for many hours (Almeida-Val and Hochachka 1995, Muusze et al. 1998; Almeida-Val et al. 2000; Sloman et al. 2006; Richards et al. 2007). The rainbow trout (*Oncorhynchus mykiss* (Walbaum, 1792)) is a salmonid that is extremely intolerant of hypoxia, exhibiting stress responses at P_{O_2} levels as high as 80 torr (Holeton and Randall 1967*a*, 1967*b*; Boutilier et al. 1988; Montpetit and Perry 1998; Lai et al. 2006). The ionoregulatory responses of these two fish to acute hypoxia were fundamentally different. Oscar exhibited pronounced reductions in both Na^+ influx and efflux rates, as well as in ammonia excretion and K^+ net flux rates at the gills in response to acute severe hypoxia (P_{O_2} = 10–20 torr; Wood et al. 2007, 2009), whereas rainbow trout exhibited exactly the opposite changes in response to acute moderate hypoxia (P_{O_2} = ~80 torr; Iftikar et al. 2010).

Our preliminary scanning electron microscope (SEM) studies of gills of the Amazonian oscar (Wood et al. 2009) and rainbow trout (Iftikar et al. 2010) were focused on gross branchial morphology and on the examination of the surface structure of mitochondria-rich cells (MRCs). They revealed that in either case, there was no gross "remodeling" at a macroscopic level, but there were rapid and oppositely directed changes in number and surface morphology of the MRCs in hypoxic water. In gills of oscar, MRCs exhibited recessed apical crypts, the number and size of which sharply decreased during hypoxic exposure, in a response that was quickly reversed upon return to normoxia (Table 1). In gills of rainbow trout, apices of MRCs were flat or slightly convex and both their numbers and individual surface areas initially increased during hypoxia (Table 1). Whereas MRC numbers later returned to normoxic levels, their apical surface area remained highly enlarged during continuing hypoxia as well as during normoxic recovery (Table 1). In both species, the mechanisms of regulation of the numbers and surface areas of MRC exposure are still unknown; only SEM was used so

Table 1. Number and apical surface area of mitochondria-rich cells in gills of the oscar (*Astronotus ocellatus*) and rainbow trout (*Oncorhynchus mykiss*) exposed to normoxia, acute hypoxia, and normoxic recovery.

	Normoxia	Hypoxia	Hypoxia	Return to normoxia
Oscar (Wood et al. 2009)				
Time at each condition (h)		1	3	3
No. of apical crypt openings/mm^2 of filament trailing edge	1691±45 D	1157±33 B	897±28 A	1473±34 C
Apical surface area of individual crypt (μm^2)	5.6±0.3 B	2.2±0.4 A	2.0±0.4 A	7.1±0.7 B
Rainbow trout (Iftikar et al. 2010)				
Time at each condition (h)		1	4	6
No. of apical crypt openings/mm^2 of filament trailing edge	3172±196 A	4090±236 B	2619±203 A	3013±242 A
Apical surface area of individual crypt (μm^2)	19.4±1.6 A	60.7±6.0 C	42.3±3.3 B	38.2±3.2 B

Note: Values are means ± SE (N = 6). Within a category, mean values sharing the same letter are not significantly different ($P \leq 0.05$).

internal subcellular changes were not investigated, and PVC and MC responses were not examined in these studies.

The present investigation was performed to provide a more comprehensive investigation of the morphological responses of the gills of oscars and rainbowtrout, building on the studies of Wood et al. (2009) and Iftikar et al. (2010). Transmission electron microscopy (TEM), light microscopy (LM), and more extensive SEM observations were employed to examine the three major types of cells comprising the gill epithelium in oscar and rainbow trout, two species that differ in their response to hypoxia. Our hypotheses were (*i*) hypoxia affects the ultrastructure, size, and shape of MRCs; (*ii*) PVCs stretch and retract their surfaces to cover and uncover apices of MRCs in response to hypoxic exposure and recovery; and (*iii*) MCs respond to hypoxic exposure.

Materials and methods

Experimental animals

Adult oscars were obtained from Sitio dos Rodrigues (Km 35, Rod. AM-010, Brazil) and held for approximately 1 month prior to experiments at the Ecophysiology and Molecular Evolution Laboratory of the Instituto Nacional de Pesquisas da Amazonia (INPA), in Manaus, Brazil. Fish mass ranged from 67 to 226 g. Fish were held with natural photoperiod in 500 L tanks, where they were fed a daily 1% ration of commercial pellets (Nutripeixe Tr 36, Purina, Sao Paulo, SP, Brazil) until feeding was suspended 48 h before experimentation. The holding and experimental water was typical Amazonian soft water taken from a well on the INPA campus (concentrations of 35 μmol·L^{-1} Na^+, 36 μmol·L^{-1} Cl^-, 16 μmol·L^{-1} K^+, 18 μmol·L^{-1} Ca^{2+}, 4 μmol·L^{-1} Mg^{2+}; 0.6 mg·L^{-1} dissolved organic carbon; pH 6.5) with partial recirculation and continuous filtration at 28 ± 3 °C. All experimental procedures complied with Brazilian and INPA animal care regulations.

Adult rainbow trout were obtained from Humber Springs Trout Farm in Orangeville, Ontario, Canada. Fish mass ranged from 150 to 250 g. The trout were acclimated for at least 2 weeks to 15 ± 0.5 °C in flowing dechlorinated Hamilton tap water, which served as the experimental medium (concentrations of 600 μmol·L^{-1} Na^+, 700 μmol·L^{-1} Cl^-, 50 μmol·L^{-1} K^+, 1000 μmol·L^{-1} Ca^{2+}, 300 μmol·L^{-1} Mg^{2+}, pH 8.0; concentration of 3.0 mg·L^{-1} dissolved organic carbon) under a 12 h light : 12 h dark photoperiod. Fish were fed a commercial fish feed (2% ration) every 2 days until feeding was suspended 48 h before experimentation. Animals were cared for in accordance with the principles of the Canadian Council on Animal Care and protocols were approved by the McMaster Animal Care Committee.

Experimental protocols

Exposure conditions for oscar are described in detail by Wood et al. (2009) (see series 9). Oscars were allowed to settle overnight in 2.5 L Nalgene chambers with flow-through water supply. During the actual experiments, the boxes were operated as closed systems at a volume of 1.5 L. Fish were killed under normoxia (N = 6), and after 1 h of acute hypoxia (P_{O_2} = 10–20 torr; N = 6), 3 h of hypoxia (N = 6), and 3 h of normoxic recovery (N = 6). Water was renewed in between each treatment and severe hypoxia was maintained by gassing with N_2. At sacrifice, oscars were anaesthetized in 0.5 g·L^{-1} neutralized MS-222 and then killed by cephalic concussion. The second gill arch from the right-hand side of each fish was excised, quickly rinsed in water, then immediately placed in cold Karnovsky's fixative for storage at 4 °C.

Exposure conditions for rainbow trout are described in detail by Iftikar et al. (2010) (see experiment 3). Adult rainbow trout were transferred to 5 L black Plexiglas™ boxes with a flow-through water supply and left overnight. During the experiment, flux boxes were operated as closed systems at a volume of 3 L. Different groups were then killed under normoxia (N = 6), and after 1 h of acute hypoxia (P_{O_2} = ~80 torr; N = 6), 4 h of hypoxia (N = 6), and 6 h of normoxic recovery (N = 6). Water was renewed in between each treatment and moderate hypoxia was induced by an N_2/air mixture that was empirically adjusted using a gas mixing pump (Wosthoff 301a-F, Bochum, Germany). Rainbow trout were rapidly killed with a lethal dose of anesthetic (0.5 g·L^{-1} neutralized MS-222). The second gill arch from the right side was dissected out, quickly rinsed in water, and immediately fixed in cold Karnovsky's fixative. Both oscar and trout samples were later transported to San Diego State University, San Diego, California, USA, for SEM, TEM, and LM analyses.

Preparation for microscopy

The middle parts of the gills were postfixed in 1% osmium tetroxide for 1 h and examined under electron and light microscopy. The parts of the gill arches used for SEM study were dehydrated in a series of ascending concentrations of ethanol from 30% to 100%, critical-point dried with liquid CO_2, mounted on stubs, sputter-coated with gold–palladium,

Fig. 1. Transmission (TEM) and scanning (SEM) electron micrographs of the apical crypts of MRCs in the filamental epithelium of the oscar (*Astronotus ocellatus*) exposed to normoxia (A), 1 h of acute hypoxia (B–C), 3 h of acute hypoxia (10–20 torr; 1 torr = 133.3224 Pa) (D), and after 3 h of recovery in normoxic water (E–F). (A) Normoxia. TEM of a shallow apical crypt with wide opening. Note numerous microvesicles in the subapical zone of cytoplasm, and mitochondria and tubular reticulum distributed below. (a, inset of A) SEM of a shallow apical crypt. Complex sieve-like surface pattern is composed of interdigitated and fused microplicae. (B) 1 h of hypoxia. TEM of a recessed MRC partially covered by PVCs. Note small opening and chamber-like structure of a deep apical crypt and few subapical microvesicles. (b, inset of B) SEM of a small apical crypt. Mucus seen on the PVC surface (black asterisk) and within the crypt (white asterisk). (C) 1 h of hypoxia. TEM of an apical crypt of an MRC completely covered by flanks of PVCs. Fused and interdigitated cytoplasmic projections give the crypt a sponge-like appearance. (D) 3 h of hypoxia. TEM of a deep flask-like apical crypt with a small opening. (d, inset of D) SEM of a small and deep apical opening of an MRC. (E) 3 h return to normoxia. TEM of apical crypt with a large apical opening. (e, inset of E) SEM of a large apical crypt masked by mucus (white asterisk). Black asterisk designates patches of mucus attached to the microridges of PVC. (F) 3 h return to normoxia. TEM of a deep apical crypt with a wide opening and chamber-like compartments. The subapical cytoplasm is almost free of microvesicles. (f, inset of F) SEM of the MRC. Note the wide MRC apical opening, a complex surface structure made by interdigitated microplicae, and thin film of mucus on the PVC surface (black asterisk). AC, apical crypt; M, mitochondria; MRC, mitochondria-rich cell; PVC, pavement cell; TR, tubular reticulum. Whitehead arrows indicate subapical microvesicles and blackhead arrows indicate intercellular junctions. Scale bars = 1 μm.

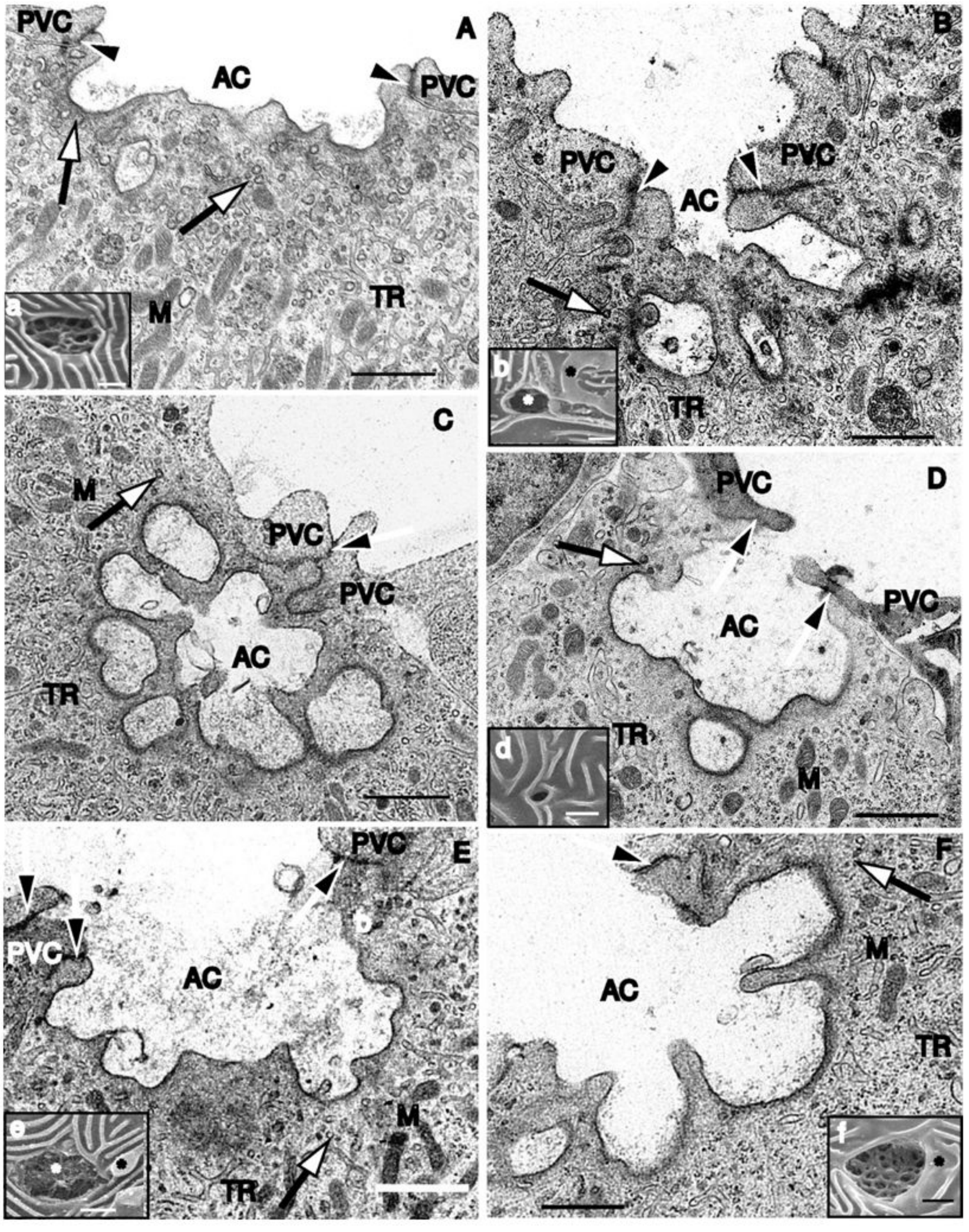

Table 2. Morphometric characteristics of cells in gills of the oscar (*Astronotus ocellatus*) exposed to normoxia, acute hypoxia (10–20 torr; 1 torr = 133.3224 Pa), and normoxic recovery.

		Hypoxia		
	Normoxia	1 h	3 h	Return to normoxia (3 h)
Mitochondria-rich cells (MRCs)				
Cross-sectional area of individual cell (μm²)	51.3±1.8 C	39.0±1.4 A	36.9±1.3 A	44.1±1.6 B
Depth of individual apical crypt (μm)	0.9±0.1 A	1.9±0.1 B	2.8±0.1 C	2.4±0.1 C
Diameter of individual apical opening (μm)	3.5±0.2 B	1.3±0.1 A	1.1±0.1 A	3.8±0.2 B
No. of microvesicles per cell profile	42±5 A	21±4 B	19±3 B	31±4 C
Pavement cells (PVCs)				
Surface area of individual cell (μm²)	103.9±5.9 A	124.2±5.5 B	126.3±7.7 B	113.9±5.8 AB
Density of microridges per test grid	83±3 C	45±2 A	43±3 A	69±3 B
Mucous cells (MCs)				
No. of MC openings/mm² on filament trailing edge	4 71±28 A	509±34 AB	570±35 AB	579±34 B
Cross-sectional area of individual MC1 (μm²)	38.2±1.4 A	43.6±1.9 AB	53.7±1.8 C	47.8±2.3 BC
Cross-sectional area of individual MC2 (μm²)	29.4±0.5 C	28.9±0.5 C	24.7±0.5 A	26.5±0.4 B

Note: Values are means ± SE ($N = 5$). Within a category, mean values sharing the same letter are not significantly different ($P \leq 0.05$).

and examined with a Hitachi S 2700 electron microscope (Hitachi, Tokyo, Japan) at the accelerating voltage of 20 kV. Samples used for TEM and LM were dehydrated in a graded ethanol–acetone series to 100% acetone and embedded in Epon epoxy resin. Semi-thin (1 μm) and ultra-thin (60–70 nm) sections were prepared parallel to the long axis of the filaments and cut with an ultra-microtome (EM-Leica microtome, Bannockburn, Illinois, USA). Semi-thin sections for LM analyses were mounted on glass slides, stained with 0.5% methylene blue, and examined in a Nikon Eclipse E200 microscope (Nikon, Melville, New York, USA). Ultra-thin sections for TEM analyses were mounted on copper grids, double-stained with 2% uranyl acetate, followed by 1% lead citrate, and examined in a Tecnai 12 transmission electron microscope (FEI) at an accelerating voltage of 80 kV.

Morphometry

Several major parameters of the gill filamental epithelium were measured in five fish from each treatment. (1) The cross-sectional areas of individual MRCs were measured in both oscars and rainbow trout on five randomly selected thick sections for each of five fish under magnification × 600 on light microscope slides. (2) The depth of individual apical openings of MRC crypts and (3) the diameter of individual apical openings in oscars only were measured on four randomly selected cells of each of five fish on TEM microphotographs under magnification × 5400. (4) The number of microvesicles per MRC profile in oscar and rainbow trout was counted in eight cells for each of five fish for each species under magnification × 11 000. (5) The surface areas of individual PVCs in oscars and rainbow trout were measured on three randomly selected cells from each of five fish on SEM microphotographs under magnification × 5000. (6) The density of microridges on the PVC surface was calculated in oscars and rainbown trout on three randomly selected cells from each of five fish as the number of intercepts of microridge profiles with a segment of test grid superimposed on the SEM microphotographs at a magnification × 5000. (7) The number of openings of MCs per mm² was calculated on five randomly selected areas for each of five fish on the trailing edge of the filamental epithelium on SEM microphotographs under magnification × 2000. (8) The cross-sectional areas of individual MCs were measured on five randomly selected thick sections for each of five fish under magnification × 600 on light microscope slides.

Note that for all surface-area measurements, we tilted our samples in a such a way that each measured cell was positioned "en face", i.e., so that the full cell surface was visible to us. The present morphometric measurements complemented the previously published measurements of Wood et al. (2009) and Iftikar et al. (2010) summarized in Table 1.

Statistical analysis

All data are reported as means ± 1 SE (N = number of fish). Relationships within each species were assessed by one-way ANOVAs, followed by Bonferroni multiple comparison tests. A significance level of $P \leq 0.05$ was used throughout.

Results

Oscar in normoxia

TEM revealed that MRCs were large elongated cells with small and shallow apical crypts containing a few thick cytoplasmic projections (Fig. 1A; Table 2). Interdigitated folds of apical membrane (microplicae) seen by SEM gave the crypts' surfaces a sieve-like appearance (Fig. 1*a*). The MRCs exhibited a light cytoplasmic matrix where numerous mitochondria were associated with an extensively branched tubular reticulum (Fig. 2A). Abundant microvesicles were distributed under the apical membrane (Fig. 1A; Table 2). The junctional complexes typically observed under normoxia included a tight junction (0.3–0.4 μm) and one or two small desmosomes that linked MRCs to neighboring PVCs (Fig. 2C). The large polygonal surface of the leaf-like PVCs had long unbranched and concentrically arranged microridges separated by narrow microgrooves (Fig. 2E; Table 2).

Fig. 2. Transmission electron micrographs of MRCs (A–B) and intercellular junctions between MRC and PVC (E–G), and scanning electron micrographs of PVCs (E–H) in the gills of the oscar (*Astronotus ocellatus*) exposed to normoxia, acute hypoxia (10–20 torr; 1 torr = 133.3224 Pa), and recovery in normoxic water. (A) Normoxia. Cytoplasm of MRC contains numerous large mitochondria associated with branched tubular reticulum. (B) 3 h return to normoxia. Note slightly enlarged mitochondria and less branched tubular reticulum. (C) Normoxia. Intercellular junctional complexes composed of a long tight junction and two desmosomes. (D) 3 h return to normoxia. Junctional complex with shorter tight junction. (E) Normoxia. Surface pattern of PVC showing long, unbranched, and concentrically arranged microridges separated with narrow microgrooves. (F, G) 1 h and 3 h of hypoxia exposure, respectively. Note the reduction of surface relief to a large smooth central area and a few microridges at the edge of the cell. (H) 3 h return to normoxia. Note partial restoration of microridge density and contraction of smooth central area. D, desmosome; M, mitochondria; MRC, mitochondria-rich cell; PVC, pavement cell; TJ, tight junction; TR, tubular reticulum. Scale bars = 1 μm (A, B), 0.2 μm (C, D), and 5 μm (E–H).

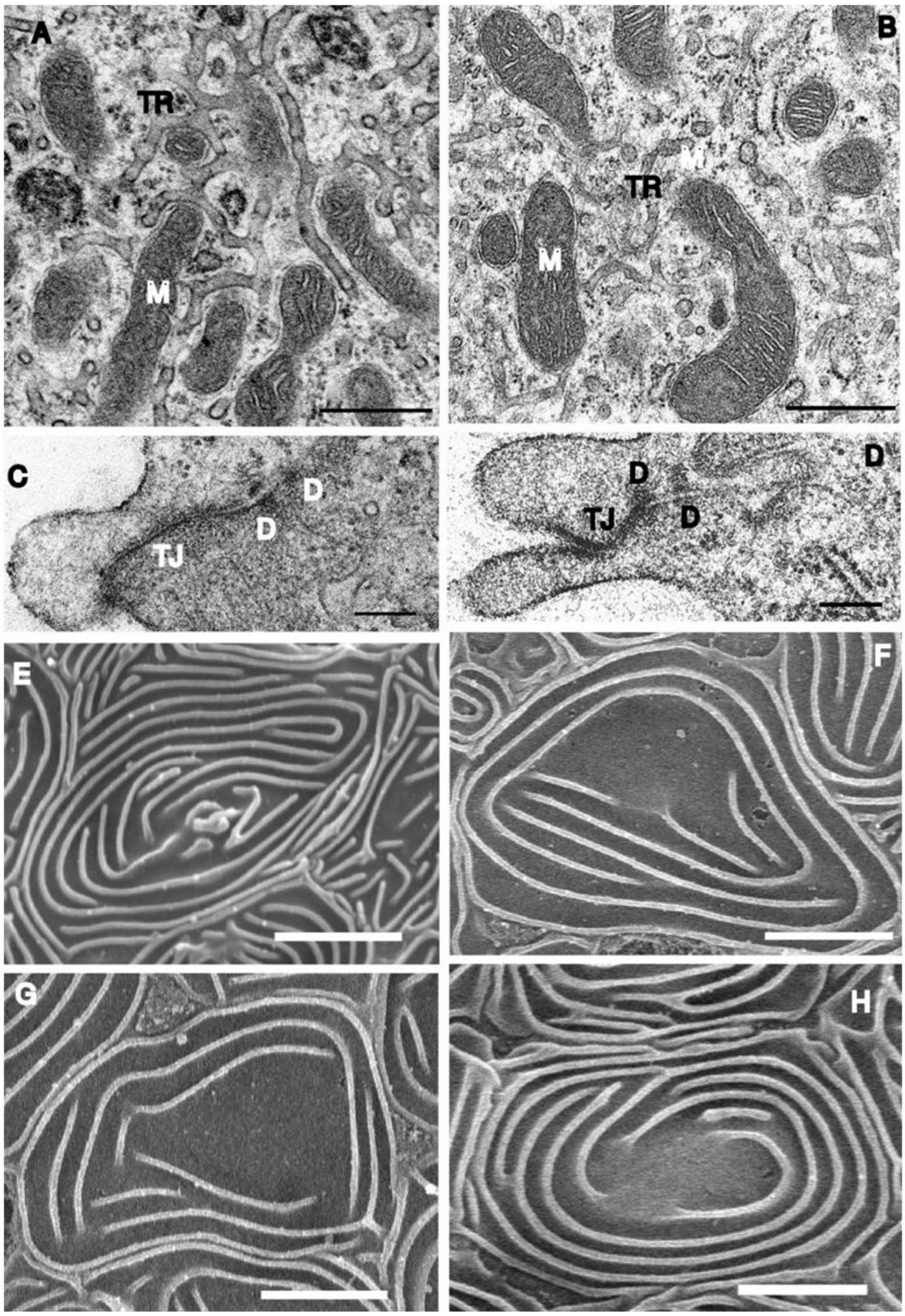

Fig. 3. Transmission electron micrographs of two types of mucous cells in the gills of the oscar (*Astronotus ocellatus*) exposed to normoxia (A–C), 1 h of acute hypoxia (10–20 torr; 1 torr = 133.3224 Pa) (D), and after 3 h of recovery in normoxic water (E, F). (A, B) Normoxia. Typical form of the type 1 mucous cells (MC1s) exposed to the water, with cytoplasm filled with large granules of low electron density (double black asterisks) (A) and the MC1 form found in the border region between filamental and lamellar epithelium, with cytoplasm containing large mucous granules of medium electron density (black asterisk) and smaller granules of high electron density (white asterisk). (C) Normoxia. Type 2 mucous cell (MC2s) in the inner layer of the filamental epithelium. The approximately round cell is filled with small elongated granules of extremely high electron density (double white asterisks). (D) 1 h of hypoxia. Note large granules of low electron density (double black asterisks) and smaller granules of medium electron density (black asterisk) within the goblet-shaped MC1. (E) 3 h return to normoxia. MC1 contains mostly large granules of medium (black asterisk) and low (double black asterisk) electron density. (F) 3 h return to normoxia. MC2 is more elongated than in the control (C) with larger and less dense granules. Note the apical crypt of the MRC located in the upper layer of filamental epithelim. AC, apical crypt; ER, endoplasmic reticulum; GA, Golgi apparatus; MRC, mitochondria-rich cell; N, nucleus. Scale bars = 1 μm.

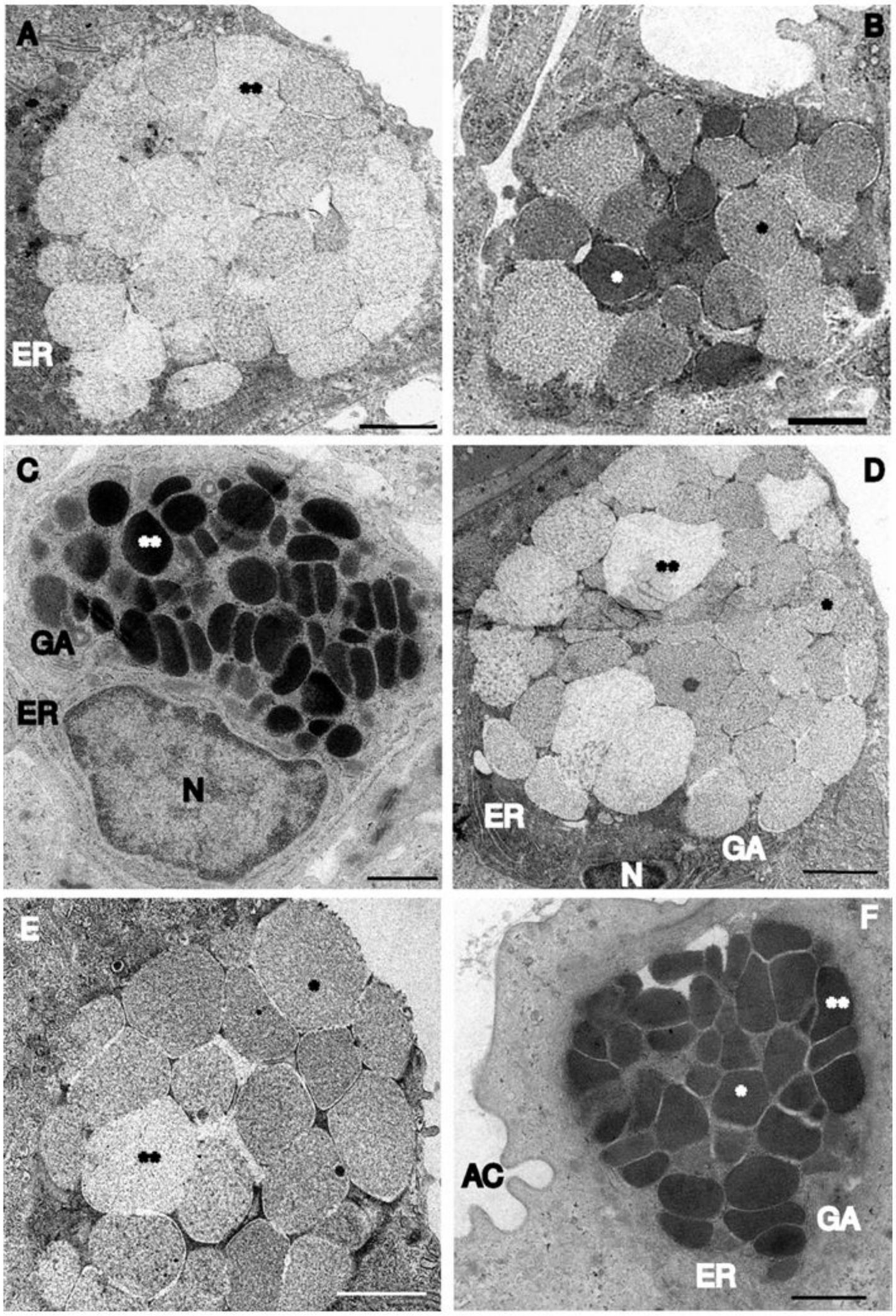

Fig. 4. Transmission (TEM) and scanning (SEM) electron micrographs of apices of MRCs in the filamental epithelium of the rainbow trout (*Oncorhynchus mykiss*) exposed to normoxia (A, B) and 1 h of acute hypoxia (80 torr; 1 torr = 133.3224 Pa) (C–D). (A) Normoxia. TEM of the apical part of the cluster composed of two MRCs. Note the relatively flat apical surfaces of the cells, bearing long and straight microvilli. (a, inset of A) SEM of apical surface of two-cell cluster of MRCs. MRCs are marked by one and double white asterisks. (B) Normoxia. TEM of the apical part of a solitary MRC with a slightly convex apical surface and stright microvilli. (b, inset of B) SEM of an MRC. In A and B, note numerous mitochondria and tubular reticulum and MRC–MRC and MRC–PVC intercellular junctions indicated by blackhead arrows. (C) 1 h of hypoxia. TEM of the apical part of a solitary MRC with a highly convex "dome-like" apical surface, with few knob-like microvilli and microvesicles located in the subapical zone of cytoplasm. (c, inset of C) SEM of the dome-like apical surface of a solitary MRC. Note glob of mucus discharging from the mucous cell (designated by black asterisk) and the thin film of mucus on the MRC surface. (D) 1 h of hypoxia. TEM of the apical part of a solitary MRC showing a "carpet- like" appearance with a flat apical surface bearing short and slightly ramified microvilli. Abundant microvesicles and prominent bundles of microfilaments are located beneath the apical membrane. (d) SEM of the MR surface. Note receptor cell bordering MRC. M, mitochondria; MC, mucous cell; mf, microfilaments; MRC, mitochondria-rich cell; PVC, pavement cell; TR, tubular reticulum. Whitehead arrows indicate subapical microvesicles; blackhead arrows indicate intercellular junctions. Scale bars = 1 μm (A–D) and 5 μm (a–d, insets).

As revealed by LM, MCs were less abundant than MRCs on the filamental epithelium (Table 2). Two types (MC1, MC2) could be distinguished (Figs. 3A–3C). MC1s were located in the outer epithelial layer and opened onto the epithelial surface. Most of these were large oval-to-oblong cells containing flattened basally located nuclei and their cytoplasm was packed with large (1.0–1.2 μm), uniform mucous granules of low electron density (Fig. 3A). In addition to these large, lucid granules, the MC1s located in the border region between filamental and lamellar epithelia also contained granules of medium electron density (0.8–1.3 μm) and small granules (0.3–0.5 μm) of high electron density (Fig. 3B). MC2s were revealed in the inner epithelial layers with no access to the water (Fig. 3C). These were generally smaller than MC1s (Table 2), almost circular and contained large nuclei, well-developed endoplasmic reticulum and Golgi complexes, and small either elongated (0.3–0.7 μm) or spherical (0.4–0.6 μm) granules of a high electron density (Fig. 3C).

Oscar after 1 h of hypoxia

Cells comprising the gill epithelium demonstrated a quick response to the severe hypoxia (10–20 torr). TEM revealed that apical crypts of MRCs exposed to the water became partially or completely covered by expanded flanks of neighbouring PVCs (Figs. 1B, 1C). LM measurements showed that MRCs decreased in cross-sectional area by 25% compared with those in the control normoxia gills (Table 2). Partially covered MRCs had crypts that were deeper by twofold, whereas the diameters of the apical openings were only about 35% of those seen in normoxia (Table 2). Fused cytoplasmic projections formed a few small chamber-like compartments within the crypts (Fig. 1B). By SEM, the surface structure of the crypts was barely visible owing to the depth of the crypt and small patches of mucus masking microplicae (Fig. 1*b*). MRCs completely covered by PVCs had large and almost symmetrically built multichamber crypts (Fig. 1C). No substantial changes were seen in the ultrastructure of mitochondria and tubular reticulum but there was a twofold reduction in the number of subapical microvesicles (Table 2). MRC–PVC intercellular junctions remained unchanged. PVCs showed a significant 20% expansion in their individual surface areas and a sharp 45% decrease in the density of microridges, leaving only a few on the cell edges (Table 2; Fig. 2F). MC1s became slightly enlarged, assuming a goblet shape, and contained only large mucous granules (0.9–1.4 μm) (Table 2; Fig. 3D). A film of mucus was stuck to the PVC surface and patches of mucus were seen within MRC crypts (Fig. 1*b*). No changes were found in MC2s.

Oscar after 3 h of hypoxia

As after 1 h of hypoxia exposure, the population of MRCs was represented by both partially and completely covered cells. Their individual cross-sectional areas remained 25% lower and apical crypts more than threefold deeper than in normoxia (Table 2). Apical crypts presented a flask-like shape and their openings with a few exceptions were very small and circular (Figs. 1D, 1d; Table 2). Similar to 1 h of hypoxia exposure, the subapical zone of cytoplasm contained a small amount of microvesicles (Table 2). The crypt of MRCs that were completely covered with flanks of PVs remained large. No further changes were revealed in the ultrastructure of MRCs and MRC–PVC junctional complexes. Similarly, no further changes were seen in the surface area, microridge density, or topography of PVCs (Table 2; Fig. 2G). However, approximately 20% more openings of mucous cells were observed on the filamental surface when observed by SEM. The cross-sectional area of individual MC1s increased by about 40%, whereas MC2s were reduced in size by about 15% (Table 2).

Oscar after 3 h return to normoxia

TEM revealed that the most MRCs had apices exposed on the filament surface and LM demonstrated that cells expanded in their cross-sectional area (Table 2; Figs. 1E, 1F). Diameters of apical openings increased to normoxic values while depth of crypts remained threefold deeper than in control (Table 2). Although patches of mucus masked the surface of many apical crypts (Fig. 1*e*), mucus-free crypts showed a surface design that highly resembled those found in control (Fig. 1*f*). MRC ultrastructure displayed a more fragmented tubular reticulum (Fig. 2B). The number of subapical microvesicles increased to almost twice that in hypoxic treatments (Table 2). The length of the tight junctions between MRCs and PVCs was approximately 80% of those in control and hypoxic treatments (Fig. 2D). The surface area of PVCs was slightly smaller and microridges became more dense, but the "normal" architecture of these cells was only partially restored (Table 2; Fig. 2H). MC1s remained numerous and large and were packed with huge granules (0.8–1.5 μm) of

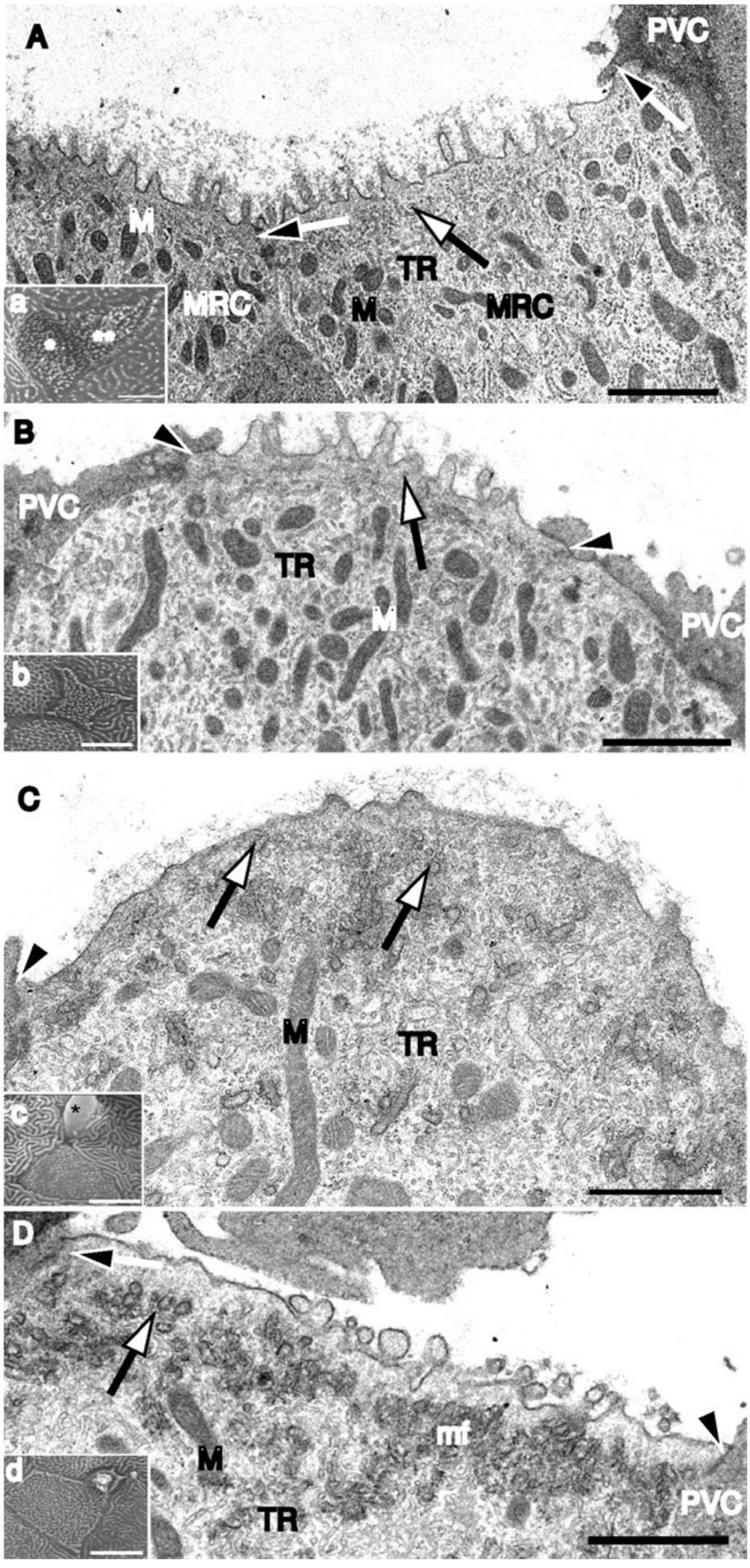
A
PVC
M
MRC
TR
M
MRC
a
B
PVC
TR
M
PVC
b
C
M
TR
c
*
D
M
mf
TR
PVC
d

Table 3. Morphometric characteristics of cells in gills of the rainbow trout (*Oncorhynchus mykiss*) exposed to normoxia, acute hypoxia (80 torr; 1 torr = 133.3224 Pa), and normoxic recovery.

		Hypoxia		
	Normoxia	1 h	4 h	Return to normoxia (6 h)
Mitochondria-rich cells (MRCs)				
Cross-sectional area of individual cell (μm^2)	49.7±2.3 A	77.2±2.2 C	63.3±2.1 B	59.6±1.8 B
Number of microvesicles per cell profile	20±3 A	32±3 B	49±4 C	24±4 A
Pavement cells (PVCs)				
Surface area of individual cell (μm^2)	129.5±5.2 B	99.4±4.5 A	140.3±5.0 BC	150.4±6.4 C
Density of microridges per test grid	341±5 A	407±7 C	353±5 AB	360±4 B
Mucous cells (MCs)				
Number of MC openings/mm^2 on filament trailing edge	547±34 A	687±33 B	760±30 B	675±39 B
Cross-sectional area of individual cell (μm^2)	58.3±1.6 A	55.0±2.1 A	71.5±2.0 B	61.1±1.6 A

Note: Values are means ± SE (N = 5). Within a category, mean values sharing the same letter are not significantly different ($P \leq 0.05$).

low and medium electron density (Fig. 3E; Table 2). MC2s remained smaller than in the normoxic treatment and contained larger and less dense granules than during hypoxia exposure (Fig. 3F; Table 2).

Rainbow trout in normoxia

In rainbow trout, MRCs were either gathered into clusters (Figs. 4A, 4a) or appeared solitary (Figs. 4B, 4b). They were large ovoid cells with apices bearing long and straight microvilli, as characterized by both SEM and TEM (Table 3; Figs. 4A, 4a). We note that the term "crypt" is not used here for the MRCs of rainbow trout, as they tended either to lie flat to the surface or to bulge out, which is in contrast to the recessed MRCs of the oscar. MRCs had light cytoplasm, abundant mitochondria, loosely branched tubular reticulum (Fig. 6A), and only a small amount of subapical microvesicles (Figs. 4A, 4B; Table 3). These cells had similar cross-sectional size to those of oscars as measured by LM (Table 3). MRCs were typically joined to PVCs with short tight junctions (0.2–0.3 μm) followed by a large desmosome (Fig. 6E). In addition, TEM revealed the presence of smaller MRCs with no access to the water below the outermost epithelial layer. PVCs had large individual surface areas, comparable with those in oscar (Table 3 vs. Table 2) but displayed a more complex surface pattern composed of long, branched, and interdigitated microridges separated by wide and shallow microgrooves (Fig. 7A). In contrast to oscar, only one type of MC could be seen by TEM, and the number of their apical openings revealed by SEM were comparable in the two species (Table 3 vs. Table 2). As seen by TEM, MCs in trout were generally round, larger than either MC1s or MC2s in oscar, and filled with mucous granules of medium electron density and varying size (0.4–1.2 μm) (Table 3 vs. Table 2; Fig. 7E). Smaller and less dense granules were also seen in these cells and some granules bore an equatorial band (Fig. 7E).

Rainbow trout after 1 h in hypoxia

The responses of MRCs of rainbow trout to acute moderate hypoxia (80 torr) were fundamentally different from those of oscar to severe hypoxia (10–20 torr). In contrast to the 25% reduction in MRC cross-sectional area seen in oscars (Table 2), there was a 55% increase in individual MRC cross-sectional area in rainbow trout as seen by LM (Table 3). Rather than being covered over by PVCs, apical exposure of MRCs greatly expanded. Most MRCs now had huge dome-like apices with highly reduced knob-like microvilli (Figs. 4C, 4c). A few MRCs exhibited a flat "carpet-like" surface pattern composed of very short and slightly ramified microvilli (Fig. 4D, 4d). Regardless of the MRC surface structure, the tubular reticulum appeared less branched and more fragmented, mitochondria were more polymorphic (Fig. 6B), and subapical microvesicles were more abundant than in controls (Figs. 4C, 4D; Table 3). Intercellular junctions were not changed. In contrast to oscar, MRCs expanded, PVC surface area was reduced by 25%, and their microridge density increased by 20% (Table 3 vs. Table 2). Wide and short microridges separated by gap-like microgrooves now tightly covered the PVC surfaces (Fig. 7B). MCs tended to become more numerous in the filamental epithelium (Table 3) and some of them even appeared on the lamellar bases. All MCs contained elongated to spherical large (0.7–1.2 μm) granules of medium electron density and smaller (0.5–0.6 μm) granules of high density (Fig. 7F). Extrusion of granules from MCs was often seen in cells opening onto the filamental surface (Fig. 4c).

Rainbow trout after 4 h in hypoxia

MRCs existed exclusively as solitary cells; clusters were not seen. Individual cross-sectional areas (by LM) were significantly reduced compared with 1 h of hypoxia exposure but remained larger than in normoxia (Table 3). There were a variety of surface patterns observed on MRCs. In most MRCs, the apices became less convex, almost smooth, or bearing rudimentary microvilli (Figs. 5A, 5a). These cells had an unusually high concentration of subapical microvesicles beneath the apical membrane (Fig. 5A; Table 3). Other MRCs had a flat surface either with a "carpet-like" design already seen after 1 h exposure, or a "ridged" surface made up of a combination of long and short microplicae (Figs. 5B, 5b). All MRCs exhibited a reduced tubular reticulum composed of thin unbranched tubules and slightly enlarged mitochondria (Fig. 6C). The individual PVC surface areas expanded and were no longer significantly different from the normoxic control areas (Table 3). The microridge density similarly returned to control values, with fine lace-like

Fig. 5. Transmission (TEM) and scanning (SEM) electron micrographs of apices of MRCs in the filamental epithelium of the rainbow trout (*Oncorhynchus mykiss*) exposed to 4 h of acute hypoxia (80 torr; 1 torr = 133.3224 Pa) (A–B) and after 6 h of recovery in normoxic water (C). (A) 4 h of hypoxia. TEM of an apex with slightly convex and almost smooth surface and a large population of subapical microvesicles. (a, inset of A) SEM of the slightly convex and almost smooth surface of an apex. Note thin film of mucus on MRC surface and opening of MC with mucous rim (designated by black asterisk) located in close proximity to the MRC. (B) 4 h of hypoxia. TEM of an apex with a flat and "ridge-like" surface. (b, inset of B) SEM of the flat and ridge-like surface of an apex. (C) 6 h return to normoxia. TEM micrograph of a cluster formed by two MRCs with carpet-like apical surfaces. (c, inset of C) SEM micrograph of two-cell cluster. M, mitochondria; mf, microfilaments; MRC, mitochondria-rich cell; PVC, pavement cells; TR, tubular reticulum. Whitehead arrows indicate subapical microvesicles; blackhead arrows indicate intercellular junctions. Scale bars1 μm (A–C) and 5 μm (a–c, insets).

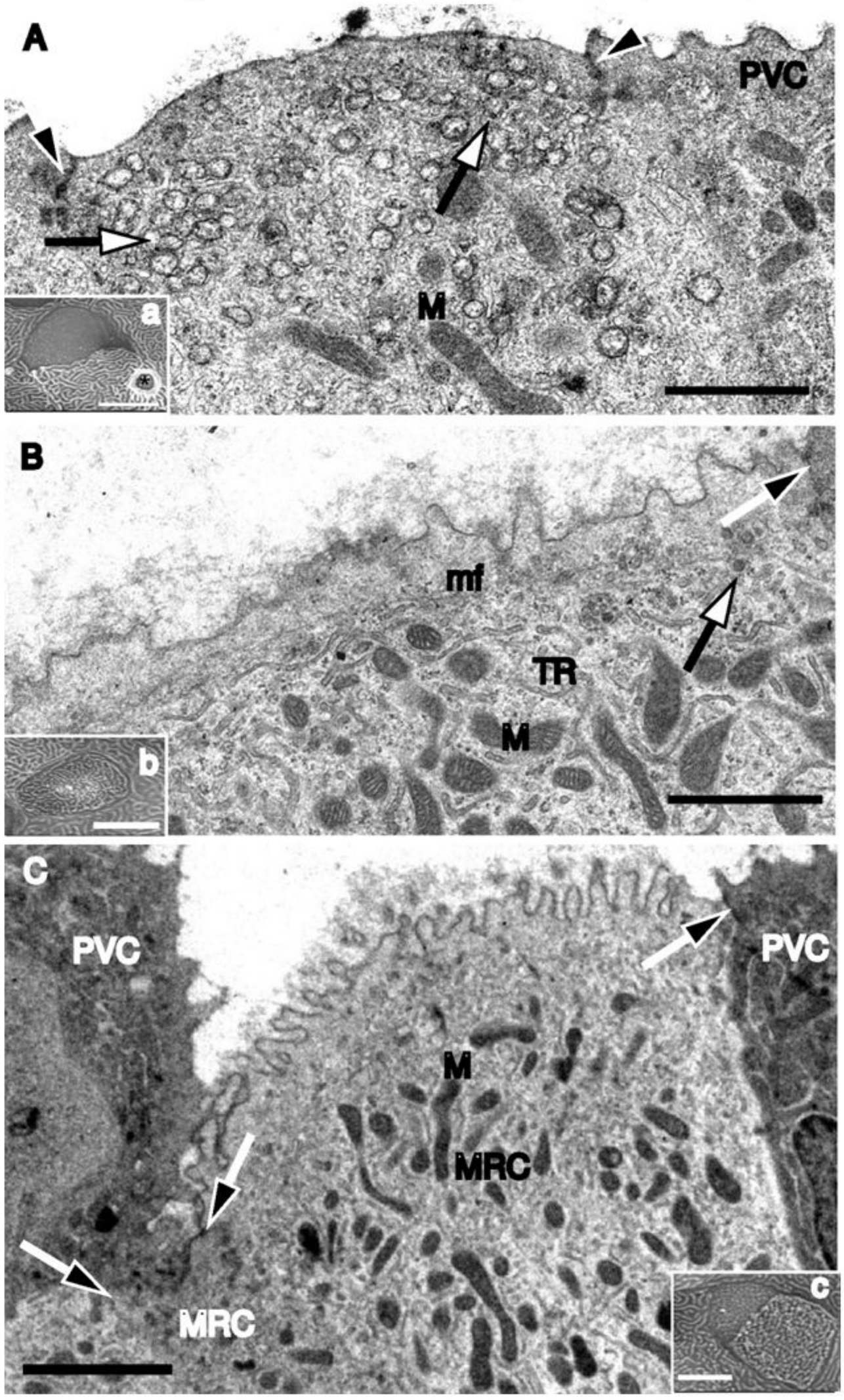

patterns (Table 3; Fig. 7C). The number of MCs opening onto the filamental surface was now significantly elevated by about 40% above normoxic control values (Table 3). Their individual cross-sectional areas as seen by LM were also significantly increased (Table 3) and they were filled with uniform granules (0.7–0.9 μm) of medium electron density (Fig. 7G). Smaller MCs were also now visible, spreading up to the mid-sections of lamellae (Fig. 7H).

Fig. 6. Transmission electron micrographs of the cytoplasm of MRCs (A–D) and intercellular junctions between MRCs and PVCs (E–F) in the gills of the rainbow trout (*Oncorhynchus mykiss*) exposed to normoxia, acute hypoxia (80 torr; 1 torr = 133.3224 Pa), and 6 h recovery in normoxic water. (A) Normoxia. Note numerous well-shaped mitochondria and elaborated tubular reticulum. (B) 1 h of hypoxia. Note polymorphic mitochondria and fragmented and less branched tubular reticulum. (C) 4 h of hypoxia. Note tubular reticulum composed of thin unbranched tubules and less numerous and enlarged mitochondria. (D) 6 h return to normoxia. Note the higher density of mitochondria and more developed reticulum than after 4 h of hypoxia exposure. (E) Normoxia. Intercellular junctional complex composed of a short tight junction followed by a prominent desmosome. (F) 6 h return to normoxia. Intercellular junctional complex. D, desmosome; M, mitochondria; MRC, mitochondria-rich cell; PVC, pavement cell; TJ, tight junction; TR, tubular reticulum. Scale bars = 1 μm (A–D) and 0.2 μm (E–F).

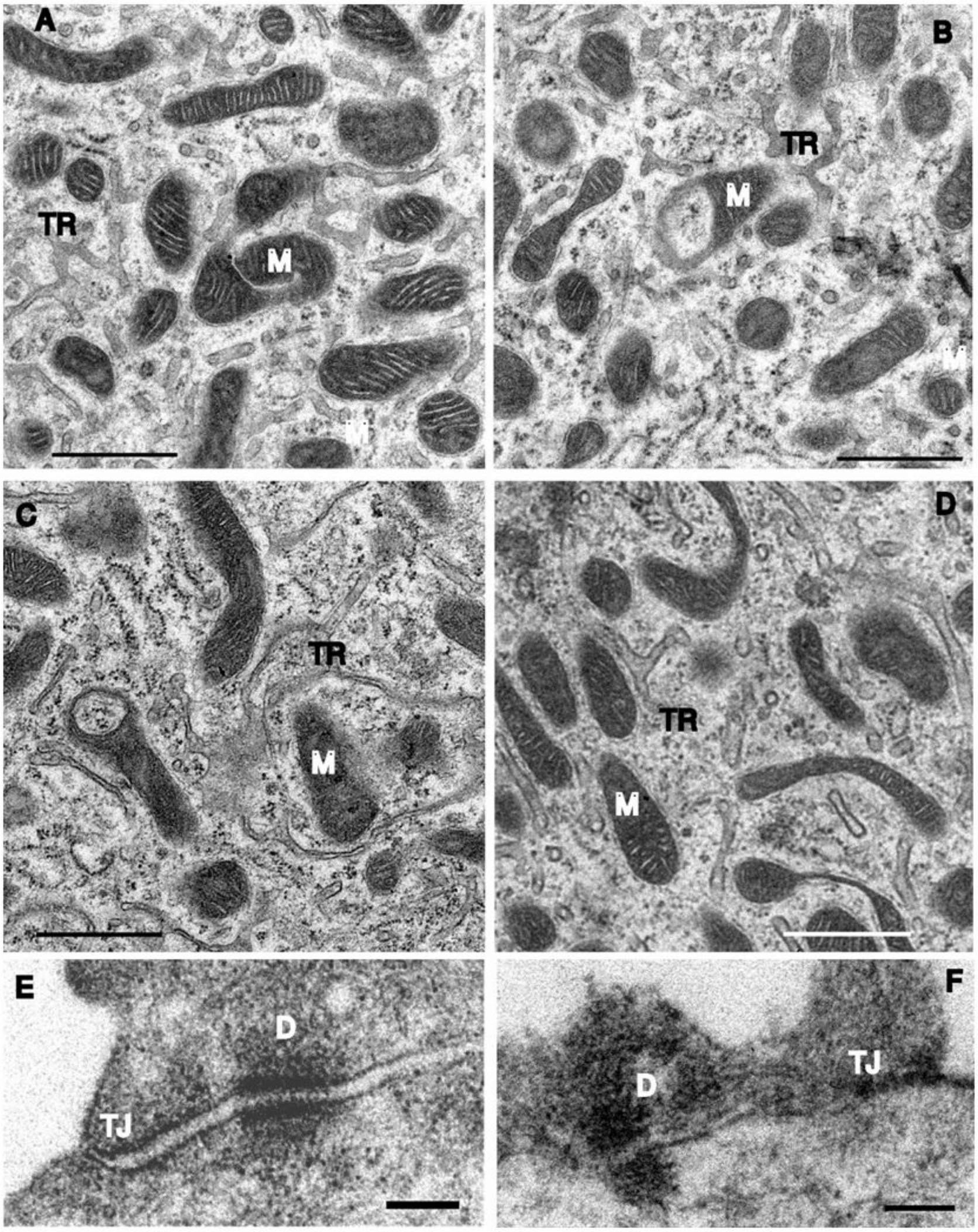

Rainbow trout after 6 h return to normoxia

In contrast to oscar, the changes seen during hypoxia in rainbow trout were not as clearly reversed after return to normoxia. For example, cross-sectional individual size (by LM) that was significantly above control values remained at the 4 h hypoxia level (Table 3). However, MRC clusters reappeared in the filamental epithelium as in normoxia and apices of solitary or clustered cells resumed their usual flat or slightly convex shape (Fig. 5C). Solitary MRCs were decorated by straight protruding microvilli, whereas the surfaces

of MRCs joined into clusters were covered by short microvilli organized in a "carpet-like" pattern (Fig. 5*c*). Mitochondria in MRCs exhibited their regular structure and the tubules of the reticulum displayed a more branched network than after 4 h exposure to hypoxia (Fig. 6D). The number of subapical microvesicles dropped to their control value (Table 3). No changes were seen in the junctional complexes (Fig. 6F). The surface areas of individual PVCs increased slightly more and now were significantly greater than the normoxic value (Table 3). Microridge density remained at the 4 h hypoxia and normoxic level (Table 3). They formed a more loosely organized pattern on the cell surface (Fig. 7D). MRC–PVC intercellular junctions remained stable (Fig. 6F). The number of MCs in the filamental epithelium fell only slightly from the 4 h hypoxia level and remained higher than normoxic values (Table 3). MCs were now typically oblong to goblet-shaped and were smaller in cross-sectional area than after 4 h hypoxia (Table 3), but MCs did not differ from control cells, containing granules of varying size, shape, and electron density (Fig. 7I).

Discussion

The freshwater gill is known to alter its morphology in response to environmental variations, thereby adapting its structure and function to suit its environment (Laurent and Perry 1991; Goss et al. 1995; Wilson and Laurent 2002; Fernandes and Mazon 2003; Kaneko et al. 2008). Acute hypoxia can now be added to the list of stressors that cause rapid morphological change, effecting dynamic and well co-ordinated responses in all three major cell types exposed to the ambient water in the filamental epithelium. In both the hypoxia-tolerant Amazonian oscar and the hypoxia-intolerant rainbow trout, morphological alterations developed rapidly, were partially reversible (more so in the oscar), and went in opposite directions.

Oscar

As originally reported by Wood et al. (2009), the number and surface area of MRCs in the Amazonian oscar sharply decreased during 3 h of hypoxia exposure and these changes were partially reversed during normoxic recovery (Table 1). In the present study, we have shown that individual cross-sectional areas of MRCs underwent similar changes, with shape and size of their apical crypts changing dramatically (Table 2). Using the MRC classification of Lee et al. (1996) and Chang et al. (2001) based on surface morphology, MRCs in oscars under normoxia were of the "shallow-basin" type; they were transformed into "deep-hole" MRCs after 1 h and 3 h of hypoxic exposure and returned to "shallow-basin" morphology after 3 h of normoxic recovery. Modification of the apical surfaces of the MRCs may involve reorganization of the cytoskeleton, membrane turnover, and (or) other intracellular alterations (Shieh et al. 2003). Exposure to hypoxia did not affect but caused a sharp decrease in the population of subapical microvesicles that was partially restored during normoxic recovery (Table 2). Thus, our first hypothesis that hypoxia affects the size, shape, and ultrastructure of MRCs was confirmed. We suppose that during hypoxia exposure, MRCs with deeply recessed small apical crypts have less area available for ion leakage through the apical membrane; this phenomenon may explain the large reduction of transcellular permeability that was observed (Wood et al. 2007, 2009). Indeed, as argued below, the reduced apical exposure of MRCs could explain the fairly uniform reduction of effluxes of many different substances that has been observed. As noted in the Introduction, it remains unclear to what extent MRCs vs. PVCs contribute to active Na^+ uptake, but it is possible that these same changes may also help explain the observed decrease in Na^+ influx during hypoxia and subsequent restoration upon return to normoxia (Wood et al. 2007, 2009). The reduced number of apical microvesicles in particular may indicate reduced trafficking of transporters or channels to the apical membrane, in accordance with the observed reductions in apparent transcellular fluxes of numerous molecules during hypoxia (Wood et al. 2009).

The present observations demonstrate that these alterations in MRC exposure were a result of a cross-relationship between PVCs and MRCs. Exposure to hypoxia caused expansion of PVCs through stretching of their apical surface at the expense of microridges (Table 2), in accordance with the interpretation of Avella et al. (2009) that PVC microridges provide a functional reserve of surface area. Expanded PVCs were able to cover and to push down neighbouring MRCs. When the protruding flanks of PVCs joined over the top, MRCs apices appeared to be buried underneath, isolated from the water, and very probably could not perform their transport functions. When PVC flanks were not completely joined together, MRCs were left with only small apical openings. Apical membranes of MRCs became recessed and folded, forming deep crypts with chambered-like internal structure. Therefore, in oscar, MRCs shrink and are covered over by pavement cells, reducing their exposure to the ambient hypoxic water and increasing the diffusion distances to the water. Upon return to normoxic water, both MRCs and PVCs exhibited high plasticity of their apical membranes. Retraction of the PVC surface allowed a large number of MRC apical crypts previously covered by PVCs to re-appear on the filamental surface, with increased apical exposure (Tables 1, 2). Therefore our second hypothesis that PVCs may stretch and retract their surface to cover and uncover apices of MRCs in response to hypoxia exposure and normoxia was found to be true in oscars.

The present observations provide additional evidence for an important morphological component in the unusual osmo-respiratory compromise of the oscar in which ionic permeability is reduced (Wood et al. 2007, 2009) while O_2 permeability is unaffected (Scott et al. 2008) during acute severe hypoxia. Based on the fluxes of several permeability markers (PEG-4000, ammonia, Na^+, K^+, ^3H_2O, urine flow—a marker of branchial osmotic water permeability), Wood et al. (2009) concluded that gills of oscar responded to severe hypoxia by a greatly reduced transcellular permeability without change in paracellular permeability. Notably, no structural alterations during hypoxia were found in the MRC–PVC tight junctions of oscar, the probable paracellular route for movement of ions. As reduced transcellular fluxes of Na^+, K^+, ammonia, urea, and water would all likely occur through membrane channel proteins, Wood et al. (2009) speculated that hypoxia causes a form of "channel arrest" in gills of oscar. This would be analogous to the "channel arrest hypothesis" proposed to explain survival of the brain and liver in

Fig. 7. Scanning electron micrographs of the surfaces of PVCs (A–D) and transmission electron micrographs of MCs in the gills of the rainbow trout (*Oncorhynchus mykiss*) exposed to normoxia, acute hypoxia (80 torr; 1 torr = 133.3224 Pa), and 6 h recovery in normoxic water. (A) Normoxia. Complex surface pattern composed of thin and highly interdigitated microridges. (B) 1 h of hypoxia. Surface pattern composed of wide microridges separated by gap-like microgroves. (C) 4 h of hypoxia. Note that the width of the microridges is decreased and that lace-like assembled microridges form a complex surface architecture. (D) 6 h return to normoxia. The PVC with a surface covered by ramified microridges is the most common morphology in the filamental epithelium. (E) Normoxia. Large MC in the filamental epithelium filled with granules of medium electron density and high electron density. Some granules show an equatorial band of lower density than the rest of the granule matrix (white arrows). (F) 1 h of hypoxia. Goblet-shaped MC on the border of the filamental and lamellar epithelium. Note the presence of mucous granules that differ in size and electron density, while large granules of medium electron density predominate. The nucleus and well-developed endoplasmic reticulum are located on the bottom of the cell. (G, H) 4 h of hypoxia. Huge MCs filled with granules of medium electron density in filamental (G) and lamellar (H) epithelia. (I) 6 h return to normoxia. Elongated MCs in the filamental epithelium. They contain huge granules of medium electron density and small granules of high electron density. ER, endoplasmic reticulum; MC, mucous cell; N, nucleus; PVC, pavement cell; RBC, red blood cell. White asterisks designated mucous granules of medium electron density; double white asterisks designated granules of high electron density. Black asterisks in A–D designated glob of mucus releasing from the MCs. Scale bars = 5 μm (A–D) and 1 μm (E–I).

other hypoxia-tolerant animals such as Crucian carp and turtles (Hochachka 1986; Boutilier 2001). If the MRCs are the primary sites of these channel-mediated fluxes, then closure of many apical crypts and narrowing of the rest by co-ordinated PVC extension and MRC recession would provide a unifying mechanism by which all transcellular fluxes could be reduced during hypoxia, rather than invoking the need for O_2 sensitivity of each different type of channel protein. The increased depth and mucification of the crypts that was observed during hypoxia could supplement this effect, further reducing effective transcellular permeability. In addition, as Na^+ influx was also reduced during severe hypoxia in the oscar (Wood et al. 2007, 2009), these results argue that the MRCs and not the PVCs are the sites of active Na^+ uptake in this species.

A recession of apical crypts and PVC-mediated decrease in MRC surface exposure formed part of a more complex morphological response ("remodeling") during hypoxic exposure in the highly hypoxia-resistant scaleless carp (Matey et al. 2008). PVC-mediated reductions in MRC exposure may be a common response mechanism to unfavorable environmental conditions, as it was also used by brown bullhead (*Ameiurus nebulosus* (Lesueur, 1819)) exposed to hypercapnia (Goss et al. 1994), Magadi tilapia (*Alcolapia alcalica* (Hilgendorf, 1905)) exposed to less alkaline water (Laurent et al. 1995), killifish (*Fundulus heteroclitus* (L., 1766)) exposed to osmotic stress (Daborn et al. 2001), and white sturgeon (*Acipenser transmontanus* Richardson, 1836) exposed to hypercarbic water (Baker et al. 2009).

In accordance with our third hypothesis, MCs clearly responded to hypoxia exposure in the oscar. Hypoxia led to a copious deposition of mucus on the surfaces of PVCs and within apical crypts of MRCs. This mucus was produced by large cells (MC1s) opening onto the epithelial surface and filled with granules of varying electron density and, probably, varying "maturity". The number and size of MC1s increased during hypoxia exposure (Table 2), and after 3 h, they contained large "mature" granules ready to be released. The population of large MC1s did not drop when fish were transferred back from hypoxic to normoxic water and mucus remained on the filament epithelium surface. The pool of smaller MC2s with small and extremely dense granules and no access to the filament surface may represent young and underdeveloped MCs. These suggestions correspond to recent data obtained on the gills of another cichlid fish, the Nile tilapia (*Oreochromis niloticus niloticus* (L., 1758)) (Monteiro et al. 2010). Using immunohistochemical approaches, Monteiro et al. (2010) revealed two subpopulations of MCs with different localization in gill epithelium (large cells in the outermost layer and smaller cells in the deeper layers, as in the oscar) and dissimilar chemical composition. They also suggested that smaller MCs may be not fully differentiated cells that were still migrating to the upper epithelial layers.

Excessive mucus production is considered a generalized response of fish gills to a number of environmental stressors, including hypoxia (Mallatt 1985; Evans 1987; Shephard 1994; Fernandes and Mazon 2003; Matey et al. 2008). It has been assumed for years that mucus may help regulate both transcellular and paracellular permeability of the gills, but direct evidence has yet to be obtained.

Rainbow trout

In contrast to the oscar, exposure to more moderate hypoxia in rainbow trout caused quick expansion of the MRCs and their transformation from "shallow-basin" to "wavy-convex" cells. Stretching of MRC's surface occurred at the expense of the outfoldings of apical membrane, the long and straight microvilli. Like microridges of PVCs, these could be used as a reserve of surface area. As originally reported by Iftikar et al. (2010), by 1 h of hypoxic exposure, the number of exposed MRCs increased 1.3 times and their individual surface area was elevated more than threefold (Table 1), making more sites available for ion transport on the gill epithelium than in normoxic fish. MRCs was highly enlarged so that their cross-sectional area increased by 55% (Table 3). Huge apices of MRCs previously covered by thin flanks of PVCs bulged out and appeared on the filamental surface, increasing the total population of exposed MRCs. In contrast to the oscar, there were ultrastructural alterations in tubular reticulum (less branching) and mitochondria (more diversity in morphology) commonly associated with less functionally active MRCs. However, subapical microvesicles became more abundant than in control. After 4 h of hypoxia, MRCs number dropped to control values, but their surface area reported by Iftikar et al. (2010) remained nearly double that in normoxia (Table 1). MRCs became smaller in cross-sectional area than after 1 h exposure (Table 3) and appeared as both "wavy-convex" and "shallow-basin" forms. Most MRCs contained obviously reduced tubular reticulum and abundant subapical microvesicles. After 6 h of

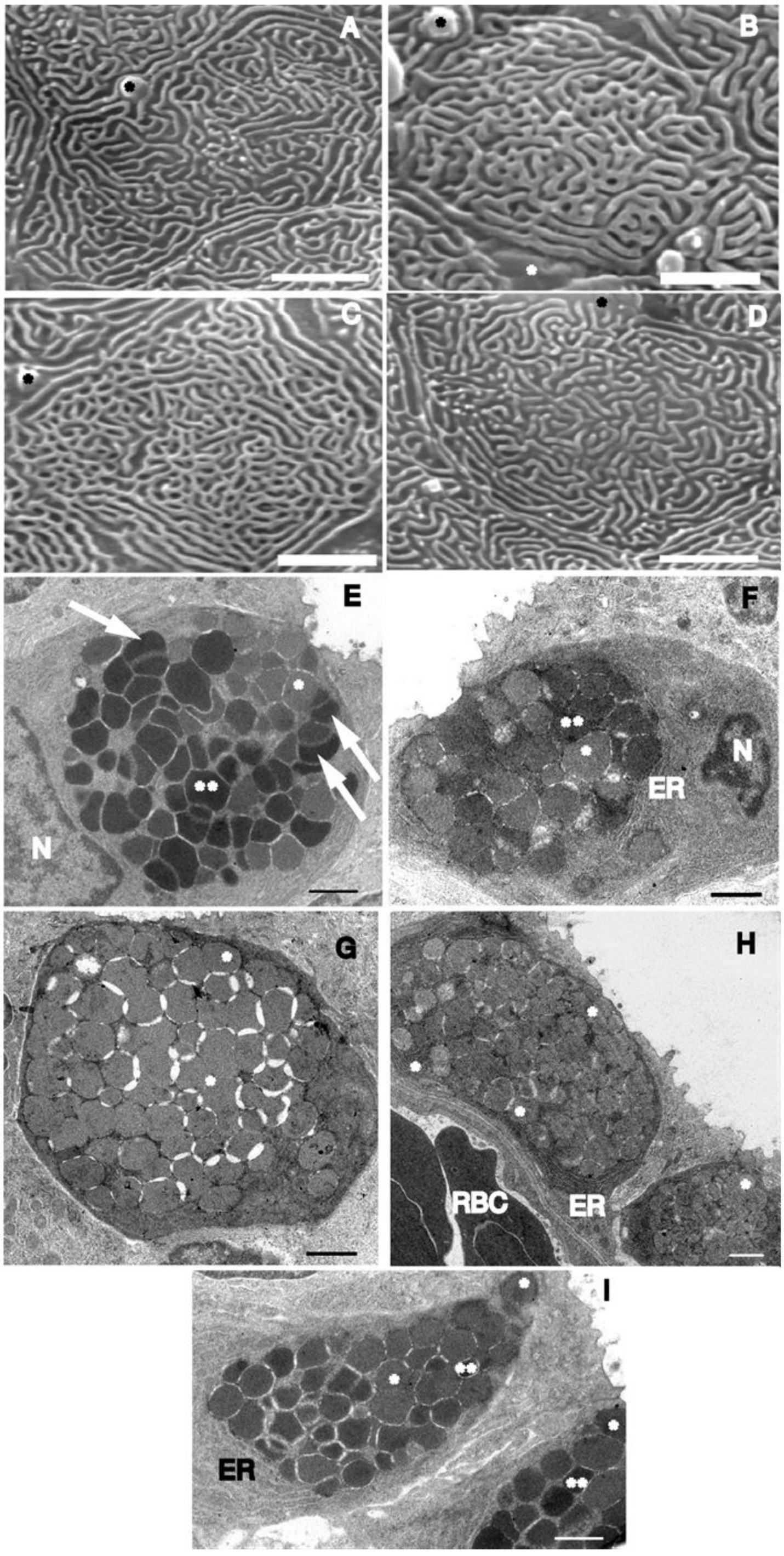
A
B
C
D
E
N
F
N
ER
G
H
RBC
ER
I
ER

normoxic recovery, changes in surface morphology and cell ultrastructure were partially reversed. Both the exposed surface area of individual MRCs (Table 1) and their individual cross-sectional areas (Table 3) remained substantially elevated relative to normoxic values. Therefore, our first hypothesis was again proven to be true: in the rainbow trout, hypoxia affected the size, shape, and ultrastructure of MRCs in the opposite direction to the effects observed in the oscar.

Iftikar et al. (2010) measured an increase in branchial Na^+ influx and efflux rates in rainbow trout during exposure to the same level of hypoxia. Using the same arguments as for the oscar, the increased density of subapical microvesicles in MRCs in particular may indicate increased trafficking of transporters or channels to the apical membrane, and the increased apical exposure of MRCs could explain the increased efflux rates of Na^+, K^+, and ammonia that were observed, assuming that these were transcellular phenomena. Increased influx and efflux rates may be also supported by a larger number of MRCs exposed to the water. Thus, the branchial epithelium of the rainbow trout exhibits clear morphological correlates of the traditional osmorespiratory compromise in which ion exchange rates are elevated at a time of increased respiratory demand (Randall et al. 1972; Nilsson 2007). Although it may seem counterintuitive that Na^+ influx (as well as efflux) should increase at a time of decreased O_2 availability, Iftikar et al. (2010) discuss several possible explanations, including changing blood flow patterns, exchange diffusion, acid–base status, and homeostatic compensation for increased Na^+ efflux; the latter has been seen during exercise (Postlethwaite and McDonald 1995).

Although changes were opposite those in the oscar, alterations in MRC exposure to the ambient water were again clearly a result of a reciprocal relationship between PVCs and MRCs. As the MRCs expanded during the first hour of hypoxia, the individual surface areas of the PVCs were reduced by 25% and their surface architecture showed an increased density of microridges (Table 3). Later, at 4 h of hypoxia and during recovery, these changes were reversed. Therefore our second hypothesis that PVCs may alter their surface to cover and uncover MRCs in response to hypoxia exposure and normoxia was also found to be true in rainbow trout.

Finally, one important similarity to the response of the oscar was the increased discharge of mucus and its marked deposition on the epithelial surface during hypoxia, proving that our third hypothesis was true in both species. MCs became larger and clearly more active. However, in trout after 4 h of hypoxia exposure, distribution of MCs was not limited to the filamental epithelium, with some migrating up the lamellar epithelium. Again, this increased mucous secretion could be a mechanism to control ion leakage and (or) support ion uptake without unduly restricting O_2 diffusion.

Concluding remarks

Overall, our results indicate that there is a rapid and important morphological component to the branchial permeability and transport responses to hypoxia in two species with very different approaches to the ionoregulatory compromise. Gills of both oscar and rainbow trout exposed to hypoxia experienced structural alterations at the tissue level (number of MRCs and MCs exposed to the ambient water), cellular level (size and shape of the MRCs, MCs, PVCs, surface structure of MRCs and PVCs), and subcellular level (number of subapical microvesicles, state of mitochondria and tubular reticulum in the MRCs). However, the oscar lives in an environment that is frequently hypoxic (Val and Almeida-Val 1995) and appears to rely more heavily on metabolic depression as a strategy for tolerating hypoxia. This strategy, in combination with the morphological changes that we have described, ensures that ionic homeostasis is maintained during severe hypoxia in the oscar (Wood et al. 2007, 2009). In contrast, the rainbow trout, which is a species normally restricted to well-oxygenated environments, invokes responses aimed at maintaining or increasing oxygen uptake resulting in augmented ion transport and leakage rates during even moderate hypoxia (Iftikar et al. 2010). The rapid yet divergent responses of pavement cells are probably an important basis for these differences between species. Other obvious morphological responses, such as those exhibited by mucous cells, are more similar between species. It is therefore clear that the gills exhibit many important responses to hypoxia, some of which we are only beginning to appreciate.

Acknowledgements

This work was funded by a Natural Sciences and Engineering Research Council of Canada (NSERC) Discovery Grant to C.M.W. and a Conselho Nacional de Pesquisa (CNPq) – Fundação de Amparo a Pesquisa do Estado do Amazonas (FAPEAM) – Programa de Apoio a Núcleos de Excelência (PRONEX) Grant to A.L.V. C.M.W. is supported by the Canada Research Chair Program and his travel to Brazil was funded in part by the International Congress of Comparative Physiology and Biochemistry. A.L.V. and V.M.F.A.-V. are recipients of research fellowships from CNPq. K.A.S. was supported by a grant from the Association for the Study of Animal Behaviour and the Royal Society (UK). G.D.B. was supported by a grant from the Research Foundation – Flanders (FWO). G.R.S. was supported by an Izaak Walton Killam Predoctoral Fellowship and was the recipient of a *Journal of Experimental Biology* travelling fellowship. We thank Maria de Nazaré Paula da Silva, Richard Sloman, Linda Daio, Sunita Nadella, Andrea Morash, and John Fitzpatrick for excellent technical assistance; Steven Barlow (SDSU) for his valuable consultations on electron microscopy; and two anonymous reviewers for constructive comments on the manuscript.

References

Almeida-Val, V.M.F., and Hochachka, P.W. 1995. Air-breathing fishes: metabolic biochemistry of the first diving vertebrates. *In* Environmental and ecological biochemistry. *Edited by* P.W. Hochachka and T.P. Mommsen. Elsevier, Amsterdam. pp. 45–55.

Almeida-Val, V.M.F., Val, A.L., Duncan, W.P., Souza, F.C.A., Paula-Silva, M.N., and Land, S. 2000. Scaling effects on hypoxia tolerance in the Amazon fish *Astronotus ocellatus* (Perciformes: Cichlidae): contribution of tissue enzyme levels. Comp. Biochem. Physiol. B Biochem. Mol. Biol. **125**(2): 219–226. doi:10.1016/S0305-0491(99)00172-8. PMID:10817909.

Avella, M., Ducoudret, O., Pisani, D.F., and Poujeol, P. 2009. Swelling-activated transport of taurine in cultured cells of sea bass: physiological adaptation and pavement cell plasticity. Am. J. Physiol. Regul. Integr. Comp. Physiol. **296**(4): R1149–R1160. doi:10.1152/ajpregu.90615.2008. PMID:19176889.

Baker, D.W., Matey, V., Huynh, K.T., Wilson, J.M., Morgan, J.D., and Brauner, C.J. 2009. Complete intracellular pH protection during extracellular pH depression is associated with hypercapbia tolerance in white sturgeon, *Acipenser transmontanus*. Am. J. Physiol. **296**(6): R1868–R1880. doi:10.1152/ajpregu.90767.2008.

Boutilier, R.G. 2001. Mechanisms of cell survival in hypoxia and hypothermia. J. Exp. Biol. **204**(18): 3171–3181. PMID:11581331.

Boutilier, R.G., Dobson, G., Hoeger, U., and Randall, D.J. 1988. Acute exposure to graded levels of hypoxia in rainbow trout (*Salmo gairdneri*): metabolic and respiratory adaptations. Respir. Physiol. **71**(1): 69–82. doi:10.1016/0034-5687(88)90116-8. PMID:3340814.

Chang, I.C., Lee, T.H., Yang, C.H., Wei, Y.Y., Chou, F.I., and Hwang, P.P. 2001. Morphology and function of gill mitochondria-rich cells in fish acclimated to different environments. Physiol. Biochem. Zool. **74**(1): 111–119. doi:10.1086/319304. PMID: 11226019.

Daborn, K., Cozzi, R.R.F., and Marshall, W.S. 2001. Dynamics of pavement cell–chloride cell interactions during abrupt salinity change in *Fundulus heteroclitus*. J. Exp. Biol. **204**(11): 1889–1899. PMID:11441031.

Evans, D.H. 1987. The fish gills: site of action and model for toxic effects of environmental pollutants. Environ. Health Perspect. **71**: 47–58. doi:10.2307/3430412. PMID:3297663.

Evans, D.H., Piermarini, P.M., and Choe, K.P. 2005. The multifunctional fish gills: dominant site of gas exchange, osmoregulation, acid–base regulation and excretion of nitrogenous waste. Physiol. Rev. **85**(1): 97–177. doi:10.1152/physrev.00050.2003. PMID:15618479.

Fernandes, M.N., and Mazon, A.F. 2003. Environmental pollution and fish gill morphology. *In* Fish adaptation. *Edited by* A.L. Val and B.G. Kapoor. Enfield Science Publishers, New Dehli and New York. pp. 203–231

Gonzalez, R.J., and McDonald, D.G. 1992. The relationship between oxygen consumption and ion loss in a freshwater fish. J. Exp. Biol. **163**(1): 317–332.

Gonzalez, R.J., and McDonald, D.G. 1994. The relationship between oxygen uptake and ion loss in fish from diverse habitats. J. Exp. Biol. **190**(1): 95–108. PMID:9317409.

Goss, G.G., Laurent, P., and Perry, S.F. 1994. Gill morphology during hypercapnia in brown bullhead (*Ichthalurus nebulosus*): role of chloride cells and pavement cells in acid–base regulation. J. Fish Biol. **45**(5): 705–718. doi:10.1111/j.1095-8649.1994.tb00938.x.

Goss, G.G., Perry, S.F., and Laurent, P. 1995. Ultrastructural and morphometric studies on ion and acid–base transport processes in freshwater fish. *In* Fish physiology. Vol. 14: Cellular and molecular approaches to ionoregulation. *Edited by* C.M. Wood and T.J. Shuttleworth. Academic Press, New York. pp. 257–283.

Greco, A.M., Gilmour, K.M., Fenwick, J.C., and Perry, S.F. 1995. The effects of softwater acclimation on respiratory gas transfer in the rainbow trout *Oncorhynchus mykiss*. J. Exp. Biol. **198**(12): 2557–2567. PMID:9320486.

Greco, A.M., Fenwick, J.C., and Perry, S.F. 1996. The effects of soft-water acclimation on gill structure in the rainbow trout *Oncorhynchus mykiss*. Cell Tissue Res. **285**(1): 75–82. doi:10.1007/s004410050622. PMID:8766860.

Handy, R.D. 1989. The ionic composition of rainbow trout body mucus. Comp. Biochem. Physiol. A Physiol. **93**(3): 571–575. doi:10.1016/0300-9629(89)90012-1.

Henriksson, P., Mandic, M., and Richards, J.G. 2008. The osmorespiratory compromise in sculpins: impaired gas exchange is associated with freshwater tolerance. Physiol. Biochem. Zool. **81**(3): 310–319. doi:10.1086/587092. PMID:18419557.

Hochachka, P.W. 1986. Defense strategies against hypoxia and hypothermia. Science (Washington, D.C.), **231**(4735): 234–241. doi:10.1126/science.2417316. PMID:2417316.

Hofmann, E.L., and Butler, D.G. 1979. The effect of increased metabolic rate on renal function in the rainbow trout, *Salmo gairdneri*. J. Exp. Biol. **82**(1): 11–23. PMID:11799679.

Holeton, G.F., and Randall, D.J. 1967*a*. Changes in blood pressure in the rainbow trout during hypoxia. J. Exp. Biol. **46**(2): 297–305. PMID:6033996.

Holeton, G.F., and Randall, D.J. 1967*b*. The effect of hypoxia upon the partial pressures of gases in the blood and water afferent and efferent to the gills of rainbow trout. J. Exp. Biol. **46**(2): 317–327. PMID:6033998.

Iftikar, F.I., Matey, V., and Wood, C.M. 2010. The ionregulatory responses to hypoxia in the freshwater rainbow trout *Oncorhynchus mykiss*. Physiol. Biochem. Zool. **83**(2): 343–355. PMID: 20095822.

Kaneko, T., Watanabe, S., and Lee, K.M. 2008. Functional morphology of mitochondrion-rich cells in euryhaline and stenohyaline teleosts. Aqua-Biosci. Monogr. **1**: 1–62. doi:10.5047/absm.2008.00101.0001.

Lai, J.C.C., Kakuta, I., Mok, H.O.L., Rummer, J.L., and Randall, D.J. 2006. Effects of moderate and substantial hypoxia on erythropoietin levels in rainbow trout kidney and spleen. J. Exp. Biol. **209**(14): 2734–2738. doi:10.1242/jeb.02279. PMID:16809464.

Laurent, P. 1984. Gill internal morphology. *In* Fish physiology. Vol. 10A: Gills. *Edited by* W.S. Hoar and D.J. Randall. Academic Press, Orlando, Fla. pp. 73–183.

Laurent, P., and Perry, S.F. 1991. Environmental effects on fish gill morphology. Physiol. Zool. **64**: 4–25.

Laurent, P., Goss, G.G., and Perry, S.F. 1994. Proton pumps in fish gill pavement cells? Arch. Physiol. Biochem. **102**(1): 77–79. doi:10.3109/13813459408996110. PMID:7516738.

Laurent, P., Maina, J.N., Bergman, H.L., Narahara, A., Walsh, P.J., and Wood, C.M. 1995. Gill structure of a fish from an alkaline lake: effect of short-term exposure to neutral conditions. Can. J. Zool. **73**(6): 1170–1181. doi:10.1139/z95-139.

Lee, T.-H., Hwang, P.-P., Lin, H.-C., and Hung, F.-L. 1996. Mitochondria-rich cells in the branchial epithelium of the teleost, *Oreochromis mossambicus*, acclimated to various hypotonic environments. Fish Physiol. Biochem. **15**(6): 513–523. doi:10.1007/BF01874924.

Mallatt, J. 1985. Fish gill structural changes induced by toxicants and other irritants: a statistical review. Can. J. Fish. Aquat. Sci. **42**(4): 630–648. doi:10.1139/f85-083.

Marshall, W.S. 2002. Na^+, Cl^-, Ca^{2+} and Zn^{2+} transport by fish gills: retrospective review and prospective synthesis. J. Exp. Zool. **293**(3): 264–283. doi:10.1002/jez.10127. PMID:12115901.

Matey, V., Richards, J.G., Wang, Y., Wood, C.M., Rogers, J., Davies, R., Murray, B.W., Chen, X.-Q., Du, J., and Brauner, C.J. 2008. The effect of hypoxia on gill morphology and ionoregulatory status in the Lake Qinghai scaleless carp, *Gymnocypris przewalskii*. J. Exp. Biol. **211**(7): 1063–1074. doi:10.1242/jeb.010181. PMID:18344480.

Mitrovic, D., and Perry, S.F. 2009. The effects of thermally induced gill remodeling on ionocyte distribution and branchial chloride fluxes in goldfish (*Carassius auratus*). J. Exp. Biol. **212**(6): 843–852. doi:10.1242/jeb.025999. PMID:19252001.

Mitrovic, D., Dymowska, A., Nilsson, G.E., and Perry, S.F. 2009. Physiological consequences of gill remodeling in goldfish (*Carassius auratus*) during exposure to long-term hypoxia. Am. J. Physiol. Regul. Integr. Comp. Physiol. **297**(1): R224–R234. doi:10.1152/ajpregu.00189.2009. PMID:19458280.

Monteiro, S.M., Fontainhas-Fernandes, A., and Sousa, M. 2010. An

immunohistochemical study of gill epithelium cells in the Nile tilapia, *Oreochromis niloticus*. Folia Histochem. Cytobiol. **48**(1): 112–121. doi:10.2478/v10042-008-0105-5. PMID:20529826.

Montpetit, C.J., and Perry, S.F. 1998. The effects of chronic hypoxia on the acute adrenergic stress response in the rainbow trout (*Oncorhynchus mykiss*). Physiol. Zool. **71**(4): 377–386. doi:10.1086/515420. PMID:9678498.

Moron, S.E., de Andrare, C.A., and Fernandes, M.N. 2009. Response of mucous cells of the gills of traira (*Hoplias malabaricus*) and jeju (*Hoplerythrinus unitaeniatus*) (Teleostei: Erythrinidae) to hypo- and hyper-osmotic stress. Neotrop. Ichthyol. **7**(3): 491–498. doi:10.1590/S1679-62252009000300017.

Muusze, B., Marcon, J., van den Thillart, G., and Almeida-Val, V.M.F. 1998. Hypoxia tolerance of Amazon fish: respirometry and energy metabolism of the cichlid *Astronotus ocellatus*. Comp. Biochem. Physiol. A Mol. Integr. Physiol. **120**(1): 151–156. doi:10.1016/S1095-6433(98)10023-5.

Nilsson, G.E. 2007. Gill remodeling in fish- a new fashion or an ancient secret? J. Exp. Biol. **210**(14): 2403–2409. doi:10.1242/jeb.000281. PMID:17601943.

Olson, K.R., and Fromm, O. 1973. A scanning electron microscopic study of secondary lamellae and chloride cells of rainbow trout (*Salmo gairdneri*). Z. Zellforsch. Mikrosk. Anat. **143**(4): 439–449. doi:10.1007/BF00306764. PMID:4589788.

Perry, S.F. 1997. The chloride cell: structure and function in the gills of freshwater fishes. Annu. Rev. Physiol. **59**(1): 325–347. doi:10.1146/annurev.physiol.59.1.325. PMID:9074767.

Postlethwaite, E., and McDonald, D.G. 1995. Mechanisms of Na^+ and Cl^- regulation in freshwater-adapted rainbow trout (*Oncorhynchus mykiss*) during exercise and stress. J. Exp. Biol. **198**(2): 295–304. PMID:9317841.

Randall, D.J., Baumgarten, D., and Malyusz, M. 1972. The relationship between gas and ion transfer across the gills of fishes. Comp. Biochem. Physiol. A Physiol. **41**(3): 629–637. doi:10.1016/0300-9629(72)90017-5. PMID:4401733.

Richards, J.G., Wang, Y.S., Brauner, C.J., Gonzalez, R.J., Patrick, M.L., Schulte, P.M., Choppari-Gomes, A.R., Almeida-Val, V.M., and Val, A.L. 2007. Metabolic and ionoregulatory responses of the Amazonian cichlid, *Astronotus ocellatus*, to severe hypoxia. J. Comp. Physiol. B Biochem. Syst. Environ. Physiol. **177**(3): 361–374. doi:10.1007/s00360-006-0135-2. PMID:17219139.

Roberts, S.D., and Powell, M.D. 2003. Comparative ionic flux and gill mucous cell histochemistry: effects of salinity and disease status in Atlantic salmon (*Salmo salar* L.). Comp. Biochem. Physiol. A Mol. Integr. Physiol. **134**(3): 525–537. doi:10.1016/S1095-6433(02)00327-6. PMID:12600661.

Scott, G.R., Wood, C.M., Sloman, K.A., Iftikar, F.I., De Boeck, G., Almeida-Val, V.M.F., and Val, A.L. 2008. Respiratory responses to progressive hypoxia in the Amazonian oscar, *Astronotus ocellatus*. Respir. Physiol. Neurobiol. **162**(2): 109–116. doi:10.1016/j.resp.2008.05.001. PMID:18555751.

Shephard, K.L. 1994. Functions for fish mucus. Rev. Fish Biol. Fish. **4**(4): 401–429. doi:10.1007/BF00042888.

Shieh, Y.E., Tsai, R.S., and Hwang, P.P. 2003. Morphological modification of mitochondria-rich cells in the opercular epithelium of freshwater tilapia, *Oreochromis mossambicus*, acclimated to low chloride levels. Zool. Stud. **42**: 522–528.

Sloman, K.A., Wood, C.M., Scott, G.R., Wood, S., Kajimura, M., Johannsson, O.E., Almeida-Val, V.M.F., and Val, A.L. 2006. Tribute to R.G. Boutilier: The effect of size on the physiological and behavioural responses of oscar, *Astronotus ocellatus*, to hypoxia. J. Exp. Biol. **209**(7): 1197–1205. doi:10.1242/jeb.02090. PMID:16547292.

Sollid, J., and Nilsson, G. 2006. Plasticity of respiratory structures — adaptive remodeling of fish gills induced by ambient oxygen and temperature. Respir. Physiol. Neurobiol. **154**(1–2): 241–251. doi:10.1016/j.resp.2006.02.006. PMID:16540380.

Sollid, J., De Angelis, P., Gundersen, K., and Nilsson, G.E. 2003. Hypoxia induced adaptive and reversible gross morphological changes in Crucian carp gills. J. Exp. Biol. **206**(20): 3667–3673. doi:10.1242/jeb.00594. PMID:12966058.

Sollid, J., Kjernsli, A., De Angelis, P., Rohr, A.K., and Nilsson, G.E. 2005. Cell proliferation and gill morphology in anoxic Crucian carp (*Carassius carassius*). Am. J. Physiol. Reg. Integr. Comp. Physiol. **289**(4): R1196–R1201. doi:10.1152/ajpregu.00267.2005.

Val, A.L., and Almeida-Val, V.M.F. 1995. Fishes of the Amazon and their environmment. Springer,-Verlag, Berlin.

Verdugo, P. 1991. Mucin exocytosis. Am. Rev. Respir. Dis. **144**(3 Pt. 2): S33–S37. PMID:1892323.

Wilson, J.M., and Laurent, P. 2002. Fish gill morphology: inside out. J. Exp. Zool. **293**(3): 192–213. doi:10.1002/jez.10124. PMID:12115897.

Wilson, J.M., Laurent, P., Tufts, P.L., Benos, D.J., Donowitz, M., Vogl, A.W., and Randall, D.J. 2000. NaCl uptake by branchial epithelium in freshwater teleost fish: an immunological approach to ion-transport protein localization. J. Exp. Biol. **203**(15): 2279–2296. PMID:10887067.

Wood, C.M., and Randall, D.J. 1973*a*. The influence of swimming activity on sodium balance in the rainbow trout (*Salmo gairdneri*). J. Comp. Physiol. A Neuroethol. Sens. Neural Behav. Physiol. **82**(3): 207–233. doi:10.1007/BF00694237.

Wood, C.M., and Randall, D.J. 1973*b*. The influence of swimming activity on water balance in the rainbow trout (*Salmo gairdneri*). J. Comp. Physiol. A Neuroethol. Sens. Neural Behav. Physiol. **82**(3): 257–276. doi:10.1007/BF00694239.

Wood, C.M., Kajimura, M., Sloman, K.A., Scott, G.R., Walsh, P.J., Almeida-Val, V.M.F., and Val, A.L. 2007. Rapid regulation of Na^+ fluxes and ammonia excretion in response to acute environmental hypoxia in the Amazonian oscar, *Astronotus ocellatus*. Am. J. Physiol. Regul. Integr. Comp. Physiol. **292**(5): R2048–R2058. PMID:17272664.

Wood, C.M., Iftikar, F.I., Scott, G.R., De Boeck, G., Sloman, K.A., Matey, V., Valdez Domingos, F.X., Duarte, R.M., Almeida-Val, V.M.F., and Val, A.L. 2009. Regulation of gill transcellular permeability and renal function during acute hypoxia in the Amazonian oscar (*Astronotus ocellatus*): new angles to the osmorespiratory compromise. J. Exp. Biol. **212**(12): 1949–1964. doi:10.1242/jeb.028464. PMID:19483013.